Characterization of Fog and Snow Attenuations for Free-Space Optical Propagation

Muhammad Saleem Awan*, Laszlo Csurgai Horwath†, Sajid Sheikh Muhammad**, Erich Leitgeb*, Farukh Nadeem*, Muhammad Saeed Khan*

*Graz University of Technology, Graz, Austria
†Budapest University of Technology and Economics, Budapest, Hungary
**National University of Computer and Emerging Sciences (FAST-NU), Lahore, Pakistan
Email: m.saleemawan@student.tugraz.at

***Abstract*— Free Space Optics (FSO) is now a well established access technology, better known for its robustness in transmitting large data volumes in an energy efficient manner. However the BER performance of a FSO ground-link is adversely affected by cloud coverage, harsh weather conditions, and atmospheric turbulence. Fog, clouds and dry snow play a detrimental role by attenuating optical energy transmitted in terrestrial free-space and thus decrease the link availability and reliability. We measured the time variation of received optical signal level during continental fog and dry snowfall over a link distance of 80 m. We perform a detailed analysis of the continental fog and dry snow attenuation results and further characterise them by presenting some useful attenuation statistics and also showing their comparison with the corresponding measured density values collected by a particle sensor device. We propose also an empirical relationship between temperature, relative humidity and optical attenuation values for the continental fog case based on standard curve fitting technique.**

***Index Terms*— Free Space Optics, cumulative distribution function (CDF) exceedance probability, visibility range, specific attenuation, particle density.**

I. Introduction

Light has an enormous potential to transmit large data volumes and the high optical frequencies make it possible to utilise very broad bandwidth in an energy-efficient manner. Optical wireless or Free Space Optics is now an established technology that accomplishes it through a well collimated high data rate optical beam using compact, low-mass terminals, while avoiding interference problems and without exhausting the radio-frequency bandwidths. Usually FSO employs modulated beams of visible or infrared light to transmit information through the terrestrial free-space for broadband communications. The main disadvantage is that a clear line of sight LOS is always required between transmitter and the receiver terminals. An additional disadvantage arises when extreme pointing, acquisition and tracking (PAT) accuracies are required to establish FSO communication link to or between mobile terminal/s.

FSO communication terminals were initially developed to bridge the "last mile" gap between optical backbone and the end users. Recently FSO is identified as an attractive alternative to complement microwave (mmW) and radio frequency (RF) links within the access network for the backhaul traffic [1, 2]. Although, FSO communication links are best served for short distances but such links are successfully tested for relatively long distance communication links (from medium to long ranges) between e.g., optical ground stations OGS and terminals in space (un-manned aerial vehicles UAVs, high altitude platforms HAPs and LEO/GEO satellites) [6, 7]. Few typical application scenarios that employ FSO to establish communication links are [3, 4, 5]:

- temporary network installation for special events and functions
- re-establishing high speed connections in case of emergency or disaster recovery situations
- bi-directional links between a relay satellite and an optical ground station including elements of a satellite constellation
- deep space or interstellar communication links
- communication links between OGS and mobile terminals in free-space like UAVs, HAPs, LEO and GEO satellites
- intra-aircraft and intra-spacecraft communication links
- ship-to-ship high data rate communications

It is now predicted that FSO will provide quantum-leap improvements especially to satellite network performance and cost besides opening up opportunities in non-traditional areas such as hybrid FSO/RF or FSO/mmW diversity; multi input multi output MIMO for the next generation of optical wireless local area network WLAN; and extreme applications having optical links extending from few mm to thousand of km. An illustration of few scenarios where FSO can be utilised to establish broadband links is illustrated in Figure 1.

A. Background

Maintaining a clear line of sight LOS between transmit and receive terminals is the biggest challenge to establish FSO links in the free-space especially in the troposphere. The LOS is diminished due to many atmospheric influences like fog, rain, snow, dust, sleet, clouds and temporary physical obstructions like e.g., birds and aeroplanes. Moreover, the electromagnetic interaction

Manuscript first received on April 10, 2009; revised version submitted on June 20, 2009. Copyright credit, project number, corresponding author: Muhammad Saleem Awan (m.saleemawan@student.tugraz.at).

doi:10.4304/jcm.4.8.533-545

of the transmitted optical signal with different atmospheric effects results in complex processes like scattering, absorption and extinction that are a function of particle physical parameters. Hence the local atmospheric weather conditions mainly determine the availability and reliability of such FSO links since there is always a threat of downtime of FSO link caused by adverse weather conditions. FSO links are also influenced by atmospheric temperature that varies both in spatial and temporal domains. The variation of temperature in the FSO channel is a function of atmospheric pressure and the atmospheric wind speed. This effect is commonly known as optical turbulence or scintillation effect and causes received signal irradiance or power fades in conjunction with the variation of temperature along the propagation path. As a result of this scintillation phenomenon, the FSO channel distance and the capacity are reduced. Thereby restricting the regions and times where FSO links can be used potentially. In order to take full advantage of the tremendous usefulness of FSO technology require a proper characterisation of different atmospheric effects influences and a meaningful interpretation of the filed measurements in such adverse conditions.

B. Contributions and Related Works

A lot of theoretical research and in situ field measurements of the atmospheric throughput attenuation has been carried out in last few years. Many theoretical models were proposed like e. g., models based on ray tracing technique, single scattering model based on Mie scattering, multiple scattering model based on radiative transfer equation theory and model based on optical depth parameter. However, most of these models were very complex and were difficult to simulate. Nowadays, a very simple empirical model that employs visibility range estimate is used to compute optical attenuations for FSO links in foggy, rainy and snowy conditions. The visibility range is measured by a system called transmissiometer and it is the distance that a parallel luminous beam travels through in the atmosphere until its intensity drops to 5% of its original value. Table 1 shows a typical range of specific attenuation values based on visibility range estimate for different fog conditions.

Recent field trials on optical signal attenuation measurements showed that fog is the most deleterious factor as optical attenuations in dense maritime fog conditions were well over 300 dB/km and in moderate continental fog conditions were up to 130 dB/km. Investigations on studying the impact of other precipitation types e.g., rain, snow and clouds on FSO links showed that optical attenuations are not non-negligible. Measurements showed rain can cause attenuations up to 25 dB/km at a rain rate of 150 mm/h [11], whereas attenuations can be up to 45 dB/km [12] in dry snowfall conditions and up to 50 dB/km [7] in clouds. Similarly, measurements showed that optical turbulence decreases exponentially with altitude and significant turbulence can be found up to 25 km altitude as most of the turbulence is created near ground and takes altitude due to convection. The optical turbulence effects are stochastic in space and time [4], with fading timescale around several milliseconds in fixed applications and reduce with carrier velocity in mobile applications. The resulting fades can exceed +/- 20 dB in extreme cases depending on the channel path and link distance [6].

Nevertheless, there are many issues to resolve, such as characterising optical attenuations for different environments, locations and atmospheric conditions (especially fog, rain, snow and clouds), substantial path losses, high shot noise levels from ambient light and restrictions on transmitter power arising from eye-safety requirements. In this contribution we present our analysis on characterisation of optical attenuations in continental fog and dry snow conditions for a terrestrial FSO link in comparison with empirical models based on visibility range estimate and discuss in detail the corresponding measured attenuations in Section IV.

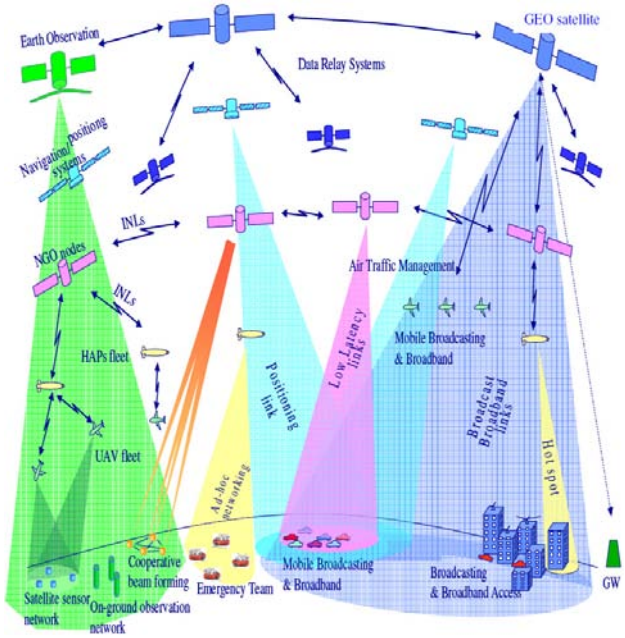

Figure 1: Few FSO application scenarios [courtesy: Integral Satcom Initiative (ISI) platform]

TABLE I

OPTICAL ATTENUATIONS BASED ON VISIBILITY RANGE ESTIMATE

Description	Visibility Range (m)	Attenuation (dB/km)
Dense Fog	40 – 70	250 – 143
Thick Fog	70 – 250	143 – 40
Moderate Fog	250 – 500	40 – 20
Light Fog	500 – 1000	20 – 9.3

C. Organization of the Paper

The remainder of this contribution is organised as follow: Section II describe our experimental measurement set-up and Section III presents a theoretical background into fog microphysics while mentioning fog and snow density measurements based on practical measurements data. Next we try to develop and explain an empirical relationship between measured temperature, relative humidity and fog attenuation values for moderate continental fog conditions based on the standard Gaussian curve fitting technique. In Section IV, we characterise

fog and snow attenuations and discuss a realistic FSO link budget. Finally, we draw conclusions in Section V.

II. Experimental Description

In this section we describe the experimental setup of measuring optical power attenuations at Graz and Milan under the moderate continental fog conditions.

A. Geographical Setting

The optical attenuation measurement campaigns took place at TU Graz campus, Graz, Austria and Politecnico di Milano, Milan, Italy. Graz and Milan are located in the temperate area at 47°04′13″N, 15°26′20″E and 45.4636°N, 9.1884°E respectively.

B. Experimental Set-up

The main purpose of our transmission measurement campaigns at Graz (Austria) and Milan (Italy) was to study and measure the transmitted optical signal attenuations primarily for fog conditions. The measurements in Graz were carried out during the winter months in 2004/05 on a 650 m link and 2005/06 on a 79.8 m link and in year 2009 we re-started again a new measurement campaign from 29th January 2009 on a 79.8 m link. Table II below, summarises the installed optical link specifications. For both 850 nm and 950 nm transmitted wavelengths, the received power is sampled once every second. The measured attenuation data, which we collected during 2005/06 and Jan. - Feb. 2009, contains some snow events too in addition to some very dense continental fog events.

The 319-m optical link in Milan (Italy) is installed within the campus Leonardo of Politecnico di Milano consists of a commercial optical link Terescope 3000 formed by two identical transceivers, which can transmit both data up to 155 Mbps and a single carrier at 785 nm. The transmitters on each side of the link are assembled in triangular shape and use three identical and independent semiconductor laser diodes having nominal output power of 10 mW and the beam divergence is 2.5 mrad. The data are sampled every 1 s. Almost continuously from 2003 to 2006, this set-up has been collecting data.

TABLE II

SPECIFICATIONS OF OPTICAL LINK AT GRAZ

Parameters	850 nm FSO Link	950 nm FSO Link
Tx wavelength	850 nm	950 nm
Tx technology	LED	LED
Rx technology	Si-APD	Si-APD
Tx avg. optical power	8 mW	1 mW per diode
Avg. radiated power	3.5 mW	4 mW
Tx aperture diameter	1x25 mm convex lens	4x25 mm convex lens
Rx aperture diameter	98 mm	98 mm
Tx divergence	2.4 degrees	0.8 degrees
Rx acceptance angle	1.7 degrees	1.7 degrees
Rx sensitivity	Min. -35 dBm	-35 dBm
Specific link margin	224 dB/km	224 dB/km
Link distance	79.8 m and 650 m	79.8 m and 650 m

III. Preliminaries

Optical signals transmitted through free-space are affected by temporal and spatial variations in the channel causing amplitude fades and frequency distortions. In this section we investigate continental fog microphysics and present our results on continental fog and dry snow density measurements. At the end of this section, we propose an empirical formula for estimating the attenuation coefficient using relative humidity and temperature values for continental fog case.

A. Fog Microphysics

Fog is composed of very fine water droplets of water, smoke, ice or combination of these suspended in the air near the Earth's surface. The presences of these droplets act to scatter the light and thus reduce the visibility near the ground surface. A fog layer is reported whenever the horizontal visibility at the surface is less than 1 km and fog can extend vertically to a height of 400 m above the ground surface up to the limit of temperature inversion. The attenuation of FSO links are in high correlation with the fog intensity, and it is particularly affected by the density and distribution of the fog particles.

Fog is found to be a superposition of five different types, each exhibiting distinct features in its spatial and temporal variability. The two most common types of fog are continental or radiation and maritime or advection fog. The main conditions favourable to the formation of fog are clear sky, and light winds [13]. Continental fog in Graz and Milan mostly occurs in winter when mild and damp air flows over a frozen or snow covered surfaces. Maritime fog can occur at any time of the year and a day or night, as it is not restricted to the conditions mentioned above. The typical fog droplet diameter ranges are from 0.17 μm to 50 μm [14-16]; mode of the droplets lying around 2 μm – 4 μm for continental (radiation) fog and around 10 μm - 12 μm for maritime (advection) fog. A cloud may also contain a good proportion of smaller water droplets, but the radii of the drops that dominate extinction and scattering are in the range of 5μm to 20μm, whereas, the limiting liquid particle diameter of a cloud is of the order of 200 μm, larger drops than this comprise drizzle or rain [15].

Simultaneous measurements of the FSO attenuation, relative air humidity and temperature are testifying that the appearance of the fog can be often detected with significant increase of the humidity (above 85 %) whilst the temperature is decreasing [17]. A typical effect of dissipation and evolution of moderate continental fog event is shown in Figs. 2(a-c). Normally, after sunset a strong cooling takes place near the earth surface through the divergence effect of long wave radiation. As the cooling increases, the relative humidity (the ratio of absolute humidity to saturation) increases until fog droplets are activated. Typically, fog formation takes place as the difference (Δ) between temperature and dew point becomes (5 °F) 3 °C, or less and as a result water vapours in the air begin to condense into liquid water form while relative humidity reaches to 100 %. The plots provided in Fig. 2 represent a time series of solar radiation, specific attenuation of optical power, relative

humidity, visibility and temperature values for a full day during which a fog event occurred at Milan, Italy. We can observe that during this fog event (240 min – 732 min) the visibility drops rapidly toward its minimum value as the relative humidity increases to more than 80 % and the temperature drops lower than approximately 5 ºC. Accordingly, dissipation of fog occurs after sunrise as the solar energy warms the surface and relative humidity drops lower than 80 % and temperature reaches more than 5 ºC.

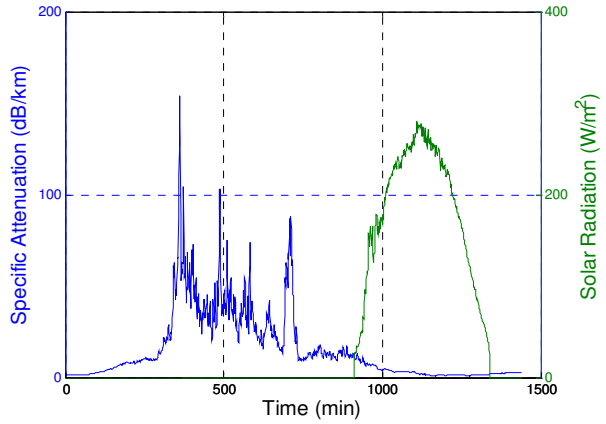

Fig. 2 (a): Specific attenuation and effect of solar radiation for a representative fog event in Milan

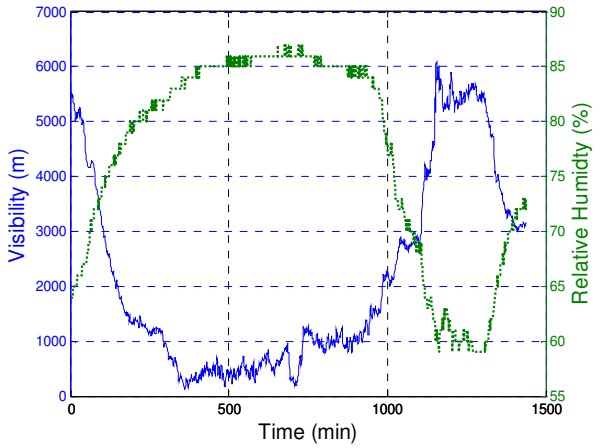

Fig. 2 (b): Effect of relative humidity on visibility during a representative fog event for Milan on a time scale.

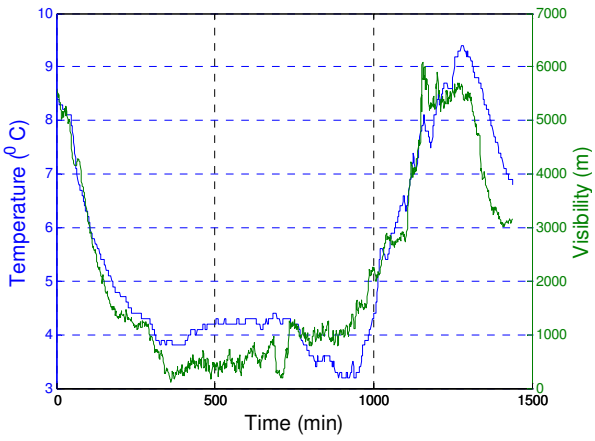

Fig. 2 (c): Effect of temperature on visibility during a representative fog event for Milan on a time scale.

B. *Principle of the fog density measurement*

To detect the appearance of the fog in the air and measure its density, Budapest University of Technology (BME) has developed a measurement device. The structure of the sensor is simpler than the other devices like nephelometers or instruments based on ray-scattering techniques. The principle of the measurement is based on the detection of reflected infrared light, which holds information about the density of fog in the air. The working principle diagram of the density measurement instrument is shown in Fig. 3.

The sensor detects particles with the size of 1 micron or higher, which is in the range of the common fog particle sizes, and calibrated to measure the density in mg/m^3. Additionally, the temperature and the relative air humidity are also measured together with the density with 1 sample/sec resolution.

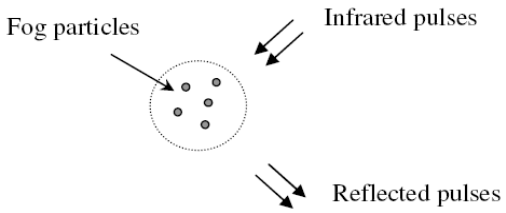

Fig. 3: Optical sensor to measure fog density

C. *Density Measurements*

The prototype of the sensor is operating since October of 2008 at TUG, Graz and BME, Hungary. During this period several fog events have been detected at both locations. In addition to fog events at Graz, three very heavy snow events also occurred during this period. It would be interesting to look into the measured density, temperature and humidity profile related to snow events. We discuss here the density profile related to fog and snow events at Graz, Austria and a fog event at Budapest, Hungary. The plot as mentioned below in Fig. 4 corresponds to a fog event at Graz that occurred on 24th January, 2009.

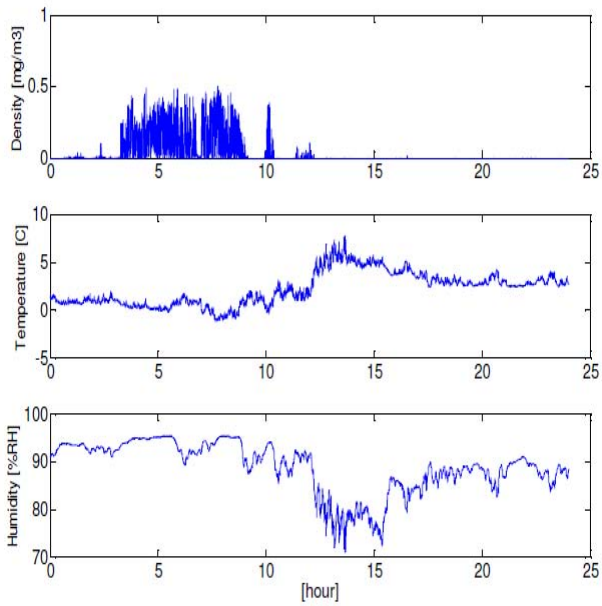

Fig. 4: Density, temperature and humidity profile for a fog event at Graz on 24.01.2009

This is a typical fog event with air humidity higher than 95% and low temperature close to 0 ºC. It is well observable that during the lower - value periods of the humidity the fog has disappeared.

In Fig. 5, we show a typical fog event that was recorded at Budapest, Hungary on 29.12.2008. It is clearly evident that the foggy periods are pairing with high humidity, but the air temperature was below the common 0 ºC. The density of fog particles reached up to 0.5 mg/m^3.

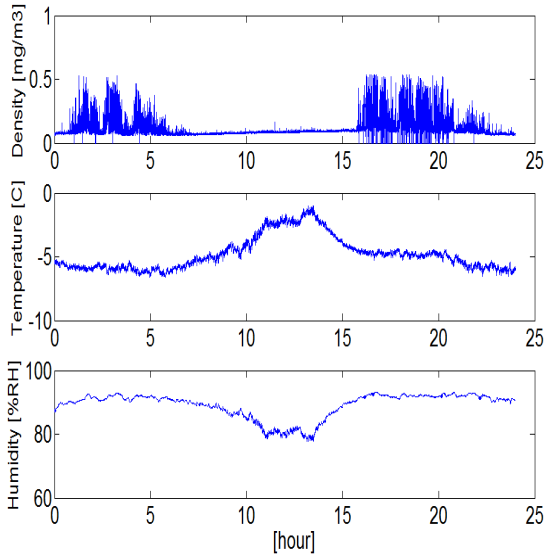

Fig. 5: Density, temperature and humidity profile for a fog event at Budapest on 29.12.2008

Another measurement is shown in the next Fig. 6, against a snow event recorded on 02.02.2009 at Graz. In this case the density shows also a deviation from the zero-level, but comparing its value with the previous example, the order of magnitude is ten times lower and it reached its maximum up to 0.03 mg/m^3. The levels of the humidity and the temperature are also non-typical for fog events. By analysing the EMT meteorological data recorded with another device close to our sensor, this event can be identified as the effect of snow coupled with very low fog intensity.

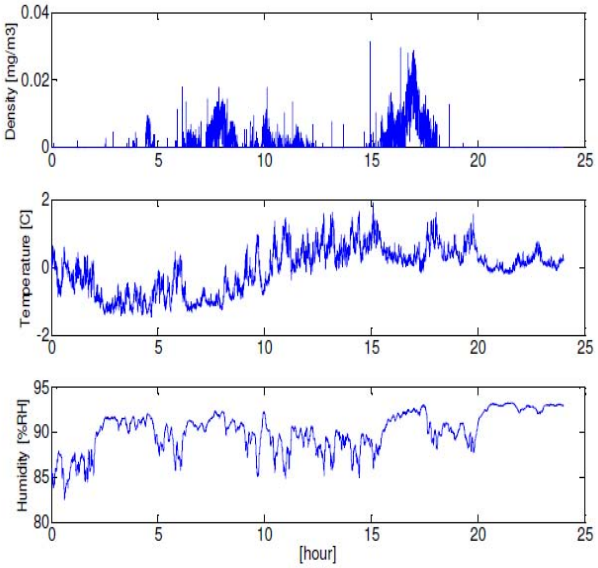

Fig. 6: Density, temperature and humidity for a snow event at Graz on 02.02.2009

Concluding the demonstrated measurement results, it has been shown that the fog sensor device can detect and measure the density of the fog particles. We noticed that the parallel measured values of temperature and humidity are in strong correlation with the fog density; however, detectable but very low level fog density could appear during snow events, as it was demonstrated in Fig. 6.

D. Relationship between relative humidity and temperature with optical power attenuation

Relative humidity (RH) and temperature (T) play an important part in the formation and dissipation of continental fog. Measurement of RH and T are simple tasks and based on their values recorded, we can approximate corresponding attenuations. However, additional information in the form of parameters like fog drop size distribution, liquid water content and fog density would further enhance the accuracy in estimating the optical attenuations. We propose here an empirical relationship between temperature, relative humidity and optical attenuation values for an optical wireless link in continental fog environments. This relationship is developed using standard curve fitting technique by employing Gaussian model which is considered a best fit in our case. The relative humidity and temperature values are plotted along x-axis in Fig. 7 and Fig. 8, respectively, while measured specific attenuation values are plotted along y-axis in both plots.

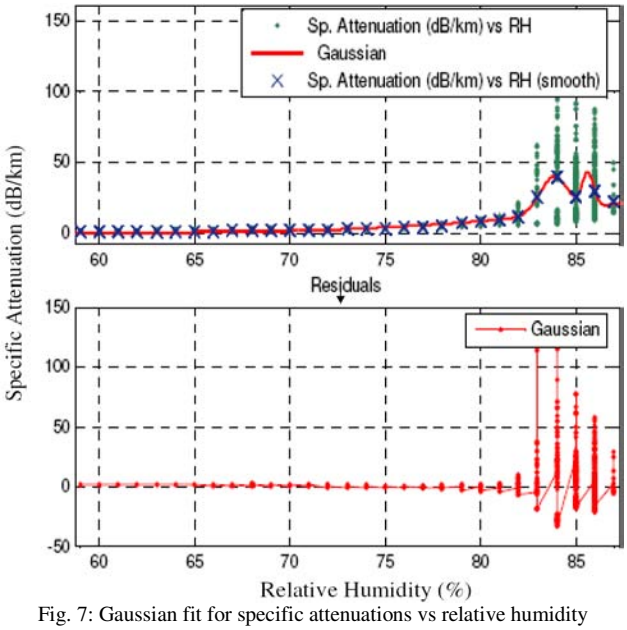

Fig. 7: Gaussian fit for specific attenuations vs relative humidity

The data values of RH-specific attenuation and temperature-specific attenuation are first smoothed (averaged) and then non-linear least square Gaussian fit is applied. There is a large scatter of attenuation values for relative humidity values between 83 % - 87 % range and temperature values between 3.5 ºC – 4.5 ºC range, as evident from Fig. 7 and Fig. 8, respectively. As the interpolation technique mentioned can not go through all the data points so we first averaged out the instantaneous variations of specific attenuation. By this way the data points are smoothed and so we applied the non-linear least square Gaussian fit. We could expect large residual errors especially for the data points lying in the above

mentioned range for temperature and RH, and it is also evident from the residuals plots as shown in lower halves of Fig. 7 and 8. The Gaussian fitting plot after smoothing the temperature-specific attenuations values and additionally showing the residual errors is presented in Fig. 8 below.

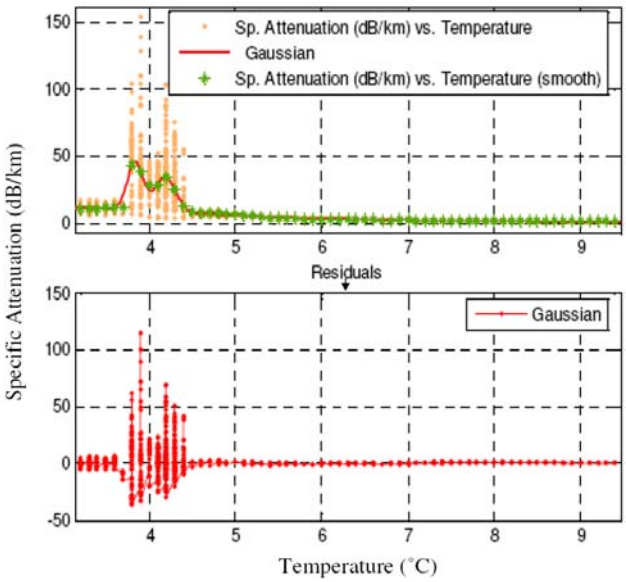

Fig. 8: Gaussian fit for specific attenuations vs temperature

It is observed that for the above mentioned relative humidity and temperature values, moderate continental fog really establishes itself and results in significantly high variations in optical power attenuations. The possible explanation to these variations in specific attenuation values can be attributed to the complex microphysical processes that vary spatially and temporally during the life cycle of the continental fog with reference to a particular location with time. The combined effect of all microphysical processes results in comparatively large fluctuations of optical signal attenuations. Quantitatively this can be observed as sum of square value of the residual errors as evident in the lower halves of the plots mentioned in Figs. 7 and 8. We applied Gaussian fitting by employing the non-linear least squares method and used the trust-region reflective Newton algorithm for this Gaussian curve fitting. The model equation is given by the following relationship,

$$\beta_{atten} = a_1 * \exp^{\left(-((x-b_1)/c_1)^2\right)} + a_2 * \exp^{\left(-((x-b_2)/c_2)^2\right)} + a_3 * \exp^{\left(-((x-b_3)/c_3)^2\right)} \quad (1)$$

Here β_{atten} is the attenuation coefficient estimated from the recorded dynamic relative humidity value x. The corresponding coefficients for relative humidity – specific attenuation and temperature-specific attenuation having 95 % confidence bounds are mentioned in Eqn. 2 and Eqn. 3, respectively. The sum of squared errors (SSE) and root mean squared errors (RMSE) arising from the residual errors is mentioned in Table III for relative humidity-specific attenuation values and for temperature - specific attenuation values in Table IV, respectively. The same model (as already given in Eqn. 1) holds true for the dynamic temperature value x.

$$\begin{aligned} a_1 &= 25.75(14.98, 36.52) \\ b_1 &= 83.85(82.69, 85.01) \\ c_1 &= 1.026(-0.7717, 2.824) \\ a_2 &= 93.89(-2568, 2756) \\ b_2 &= 113.8(-242.2, 469.9) \\ c_2 &= 21.77(-80.5, 123.6) \\ a_3 &= 24.46(-2.335\times10^5, 2.335\times10^5) \\ b_3 &= 85.64(-903.2, 1075) \\ c_3 &= 0.4174(-1501, 1502) \end{aligned} \quad (2)$$

$$\begin{aligned} a_1 &= 36.04(32.36, 39.72) \\ b_1 &= 3.839(3.826, 3.852) \\ c_1 &= 0.1298(0.09624, 0.1634) \\ a_2 &= 26.16(23.65, 28.66) \\ b_2 &= 4.189(4.171, 4.207) \\ c_2 &= 0.1722(0.1428, 0.2017) \\ a_3 &= 263.7(-7976, 8504) \\ b_3 &= -12.74(-158.4, 132.9) \\ c_3 &= 9.071(-28.11, 46.25) \end{aligned} \quad (3)$$

TABLE III

STATISTICAL PARAMETERS OF FITTING MODEL BETWEEN RELATIVE HUMIDITY AND SPECIFIC ATTENUATIONS

SSE	Rsquare	DFE	Adjrsquare	RMSE
2.809 x 10^5	*0.47594*	*1426*	*0.473*	*14.035*

TABLE IV

STATISTICAL PARAMETERS OF FITTING MODEL BETWEEN TEMPERATURE AND SPECIFIC ATTENUATIONS

SSE	Rsquare	DFE	Adjrsquare	RMSE
2.4426 x 10^5	*0.5443*	*1426*	*0.54175*	*13.088*

IV. CHARACTERISATION OF FOG AND SNOW ATTENUATIONS

In a terrestrial FSO scenario the communication transceivers are typically located in the troposphere. Troposphere is home to all kinds of weather phenomena and plays a very detrimental role for FSO communications in lower visibility range conditions mainly due to rain, snow, fog and clouds. We simulate fog, snow and rain attenuation effects using empirical models as mentioned in Equations (4), (7) and (8), respectively and the corresponding plot is shown in Fig. 9 below.

Fog attenuations can be predicted using a visibility range estimate by considering a 2 % transmission threshold (τ_{TH}) over the free space atmospheric path [13]. The fog attenuation coefficient in this case is given by,

$$\alpha_{fog}(\lambda) \cong \beta_a(\lambda) = \frac{\ln(\tau_{TH})}{V}\left(\frac{\lambda}{550}\right)^{-q} = \frac{3.912}{V}\cdot\left(\frac{\lambda}{550}\right)^{-q} \text{ [dB/km]} \quad (4)$$

Or, if we consider a 5 % transmittance threshold [13], then the fog attenuation coefficient is,

$$\alpha_{fog}(\lambda) \cong \beta_a(\lambda) = \frac{\ln(\tau_{TH})}{V}\left(\frac{\lambda}{550}\right)^{-q} = \frac{13}{V}\cdot\left(\frac{\lambda}{550}\right)^{-q} \text{ [dB/km]} \quad (5)$$

where V is visibility range in km, λ is transmission wavelength in nm. $\alpha_{fog}(\lambda)$ is the total extinction coefficient and q is the size distribution coefficient of scattering related to size distribution of the droplets. In case of clear or foggy weather with no rain or snow, we employ Kim's model approximations of the q parameter to compute the fog attenuation γ(λ), that are very accurate for the narrow wavelength range between 785 – 1550 nm [13],

$$q = \begin{cases} 1.6 & (V > 50 \text{ km}) \\ 1.3 & (6 \text{ km} < V < 50 \text{ km}) \\ 0.16V + 0.34 & (1 \text{ km} < V < 6 \text{ km}) \\ V - 0.5 & (0.5 \text{ km} < V < 1 \text{ km}) \\ 0 & (V < 0.5 \text{ km}) \end{cases} . \quad (6)$$

Kim, Kruse and Al Naboulsi (radiation fog and advection fog) models [10] are the most common empirical models used in order to predict the fog attenuations from visibility range estimate empirically. Similarly, the snow attenuations of the optical signal based on visibility range can be approximated reasonably well by the following empirical model [18],

$$\alpha_{Snow} = \frac{58}{V} \quad (7)$$

and the rain attenuations by [19],

$$\alpha_{Rain} = \frac{2.9}{V} \quad (8)$$

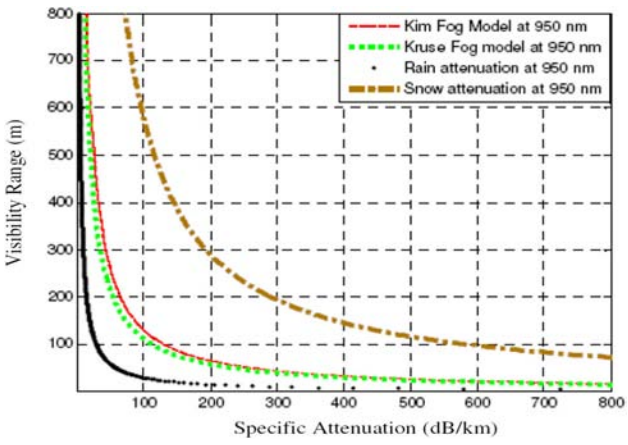

Figure 9: Simulation of empirical models for fog, rain and snow conditions for a FSO link operating at 950 nm

A. Optical Attenuations in Fog Conditions

The attenuation coefficient (α) is the sum of the absorption and the scattering coefficients from aerosols and molecular constituents of the atmosphere. The attenuation effects due to absorption can be minimised by the appropriate selection of optical wavelengths for transmission. Whereas scattering results in angular redistribution of the optical field with and without wavelength modification. The scattering effect depends on the characteristic size parameter (x_0), such that $x_0 = 2\pi r / \lambda$, where r is the size of the aerosol particle encountered during propagation. If $x_0 << 1$ the scattering process is termed as Rayleigh scattering, if $x_0 \approx 1$ then it is Mie scattering and for $x_0 >> 1$, the scattering process can then be described using Geometrical scattering theory. The scattering process for different scattering particles present in the atmosphere is summarised in Table V, below.

Transmitted optical beams in free space are attenuated most by the fog droplets mainly due to dominance of Mie scattering effect in the wavelength band of interest in FSO (0.5 μm – 2 μm). This makes fog a key contributor to optical power/irradiance attenuation; however, the attenuation contributions due to snow and rain are not negligible either. Fog droplets can induce attenuations up to 130 dB/km in moderate continental fog conditions. The attenuation levels are too high and obviously are not desirable.

TABLE V

TYPICAL ATMOSPHERIC SCATTERING PARTICLES, WITH SIZE PARAMETER AT 850 NM.

Type of particles	Radius (μm)	Size parameter (x_0)	Scattering regime
Air molecules	0.0001	0.00074	Rayleigh
Haze particles	0.01 – 1	0.074 – 7.4	Rayleigh – Mie
Fog droplets	1 – 20	7.4 – 147.8	Mie – Geometrical
Rain droplets	100 – 10000	740 – 7400	Geometrical
Snow flakes	1000 – 5000	7400 – 37000	Geometrical

The Mie scattering occurs when the fog droplets size is comparable to the transmitted optical beam size. Computation of attenuation by Mie scattering procedure is very complicated and cannot be calculated a priori for particles of complex shapes, orientations and chemical composition such as those experienced in the atmosphere. However, we make some assumptions that do not seem to have a large impact on the accuracy of the results calculated. They are: the scattered light and the incident light has the same wavelength, the particles are spherical in shape and are acting independently with a complex refractive index in space, and effects due to multiple scattering can be ignored. No experimental evidence of multiple scattering effects has been found in the case of optical transmission through moderate fog [20]. Simulations based on a model of random walk of photons through the atmosphere [21] show that in the case of thick fog (visibility less than 250 m), the path attenuation in the first optical window is a few percent smaller (on a dB scale) than the one predicted by a single scattering model.

The attenuations are predicted either theoretically by microphysical models based on the computation of

received power and the knowledge of the fog particles size distribution or through empirical relationships derived from simultaneous measurements of visibility range as mentioned in Eqn. 4, above. Fig. 10 & Fig. 11 present the time series of two representative fog events that occurred at Milan and Graz, respectively.

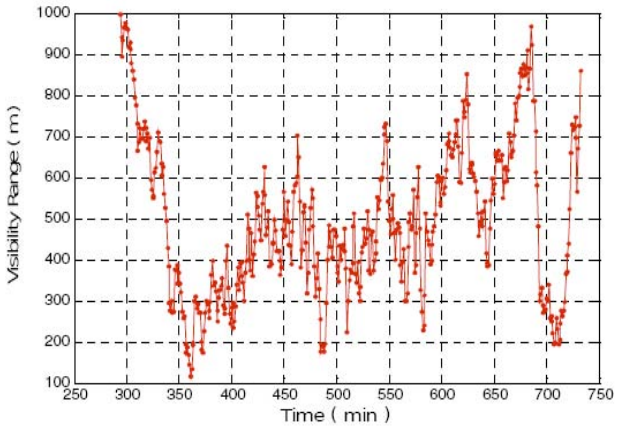

(a)

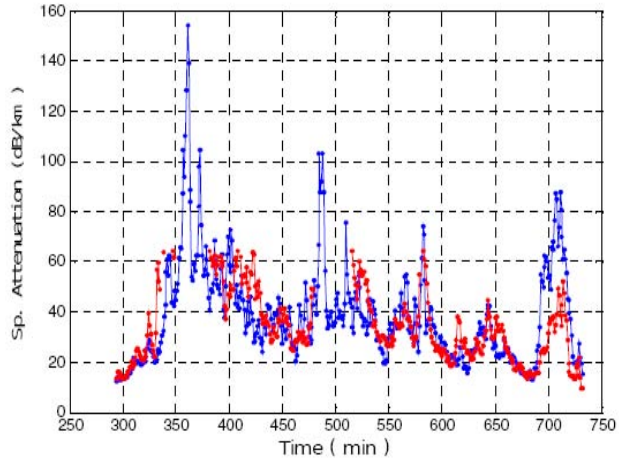

b)

Fig. 10: a). Visibility range and corresponding b). actual measured optical signal attenuations (red curve) and the attenuation as estimated from visual range (blue curve) for a representative moderate continental fog event at Milan

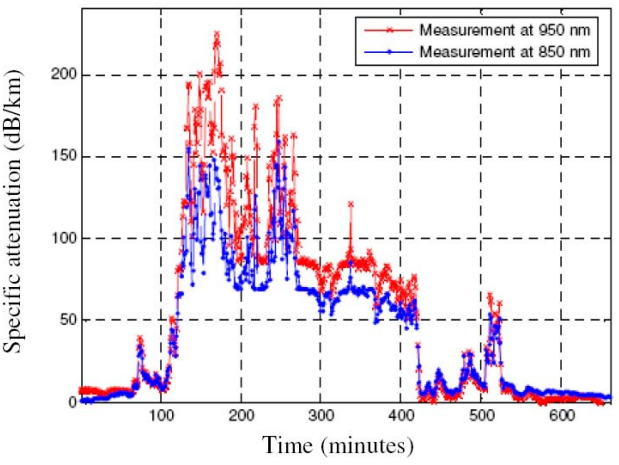

Fig. 11: Specific attenuation for 850 & 950 nm wavelengths at Graz

One can notice that the specific attenuation values as shown in Fig. 10 (b) are in strong correlation with the measured visibility range as plotted in Fig. 10 (a). The measured specific attenuation peak value of this fog event is about 154 dB/km against a visibility range of 114 m. Whereas, the measured peak value of specific attenuation is about 224 dB/km at 950 nm for the representative fog event of Graz as plotted in Fig. 11 below.

B. Optical Attenuations in Snow Conditions

We observed three major snow events on a 79.8 m FSO link at Graz; one in Nov. 2005 and the other two in Feb. 2009. The snowfall event of Nov. 2005 was the longest as it lasted from 25th – 28th Nov. 2005. The last two snow events were observed on 01st and 2nd Feb. 2009 during our recent attenuation measurement campaign on a 80 m optical link. Specific attenuation peak value of 50 dB/km was observed for the Nov. 2005 snowfall event, whereas peak attenuation values of 30 dB/km and 68 dB/km were observed against 1st and 2nd Feb. 2009 snow events, respectively. The peak value of snow attenuations can vary from event to event depending upon the snowflake size and the snowfall rate. Generally the snowflake size is larger than the rain drop size which results in much deeper fades when compared with the corresponding fades due to rain drops. Recent studies [22] reported that a snowflake size can be as large as 20 mm and it can even completely block the optical signal if the beam width is smaller than the snowflake size. The plot as shown in Fig. 12 represents the time series of specific attenuations averaged on a minute scale for all three above mentioned snow events.

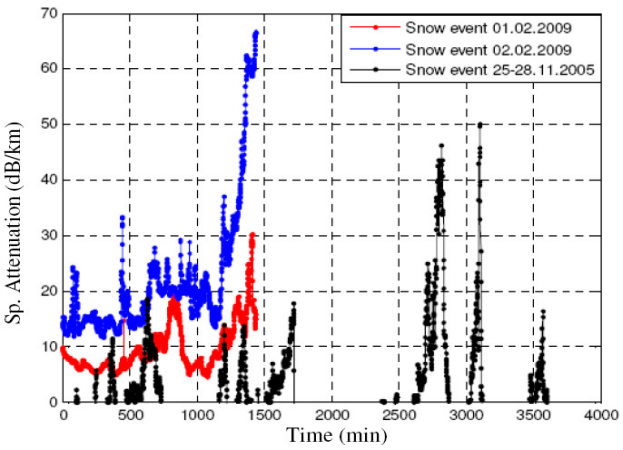

Fig. 12: Time series of three representative snow events against 950 nm transmission wavelength on a 79.8 m optical link.

C. Fog and Snow Attenuations Statistics

Reliability of FSO links is to be based on readily available long term meteorological observations for various geographical locations around the world. For FSO link design and installation the extreme attenuation determines the link availability. Our whole measurement data contains about 23 major fog events with duration more than half hour each. These moderate continental fog events are summarised and their attenuation behaviour is reported in Table VI. The last two columns of the table show optical attenuation values measured during fog with the 50 % and 99 % percentiles of the attenuation

distribution. This data shows that all but two fog events have a 99 % attenuation above it. It is important to remember that the values reported are measured on a time scale of one value per second. It is reasonable to declare here that few very dense continental fog events occurred during the measurement period of year 2005 / 2006, as the measured attenuation values on a 79.8 m optical link are quite large. It was observed that generally the atmospheric conditions were stable at large at Graz, as we noticed that a maximum temperature variation of about 10 ˚C is observed against the longest fog event (of 11th November 2005) at Graz.

TABLE VI

FOG EVENTS MEASURED AT GRAZ DURING WINTER 2005/06

ID	Initial Date	End Date	Duration	Max.	50%	90%
1.	29.09.2005	29.09.2005	1:12	81.09	13.642	78.63
2.	29.09.2005	29.09.2005	1:29	84.25	15.378	79.95
3.	29.09.2005	29.09.2005	1:40	83.94	14.921	79.31
4.	25.10.2005	25.10.2005	1:32	109.62	45.228	93.25
5.	25.10.2005	25.10.2005	1:29	113.14	43.045	95.434
6.	25.10.2005	25.10.2005	0:37	118.61	47.441	97.616
7.	26.10.2005	26.10.2005	1:31	117.8	7.108	109.64
8.	26.10.2005	26.10.2005	0:43	119.42	9.439	111.97
9.	11.11.2005	11.11.2005	4:32	55.918	11.18	52.051
10.	12.11.2005	12.11.2005	3:35	53.267	10.075	50.947
11.	22.11.2005	22.11.2005	2:03	111.8	7.318	108.490
12.	29.11.2005	29.11.2005	2:43	121.74	9.33	115.7
13.	30.11.2005	30.11.2005	1:01	112.78	8.457	109.6
14.	13.12.2005	13.12.2005	1:37	128.31	13.421	119.18
15.	09.01.2006	09.01.2006	1:11	115.5	70.837	109.77
16.	09.01.2006	09.01.2006	1:52	117.65	73.127	112.06
17.	10.01.2006	10.01.2006	3:47	118.78	44.69	115.48
18.	30.01.2006	31.01.2006	3:38	159.01	22.51	125.29
19.	31.01.2006	31.01.2006	3:07	218.92	50.121	207.96
20.	01.02.2006	01.02.2006	2:10	224.2	87.676	198.22
21.	01.02.2006	01.02.2006	2:24	213.1	84.35	197.58
22.	02.02.2006	02.02.2006	1:48	224.96	36.562	199.99
23.	03.02.2006	03.02.2006	2:16	213.94	32.02	195.46

In general, by looking at the whole attenuation data from Graz that contains 23 major fog events, the observed changes in specific attenuations were about ± 6 dB/km averaged on a second scale. A histogram of changes in specific attenuations for the representative fog event of 11th November 2005 is shown in Fig. 13, below.

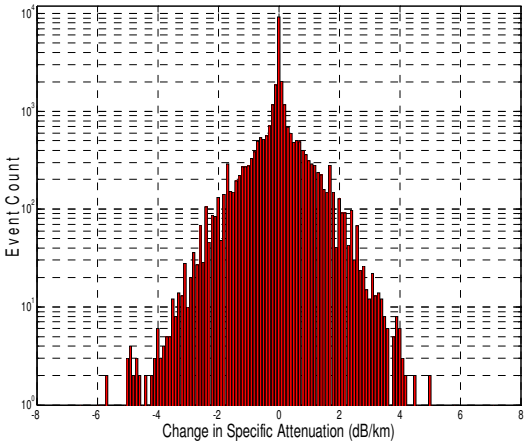

Fig. 13: A histogram of changes in specific attenuations during a representative fog event of 11.11.2005

It would be appropriate here to analyse these fog and snow attenuation results in terms of their cumulative statistics. If we denote the cumulative distribution of total attenuations by $P_{Atot}(x)$, which is the probability that - at an arbitrary time interval t_0 the total attenuation exceeds x dB so that the optical link remains unavailable. This is given by Eqn. 9,

$$P_{Atot}(x) = P\{A_{tot}(t_0) \geq x\} \qquad (9)$$

where x is the normalized link margin and its design increases the link availability. The quality of service (QoS) requirement of an FSO link is fulfilled if total attenuation A_{tot} is less than or equal to x dB. We obtain the optical link availability as expressed by Eqn. 10,

$$Availability = (1 - P_{Atot}(x)) * 100\% \qquad (10)$$

The frequency and persistence of the continental fog, like most other meteorological effects, shows a marked seasonal dependence. Especially, in winter the probability of occurrence of continental fog is much higher as relative humidity reaches more than 80 % and temperature remains close to 0 ˚C. We analyse our continental fog attenuation data, for the 80 m FSO link at Graz, consisting of five winter months (Oct. 2005 – Feb. 2006). The plot as given in Fig. 14 shows the CDF exceeded (%) for the mentioned five winter months of year 2005-06.

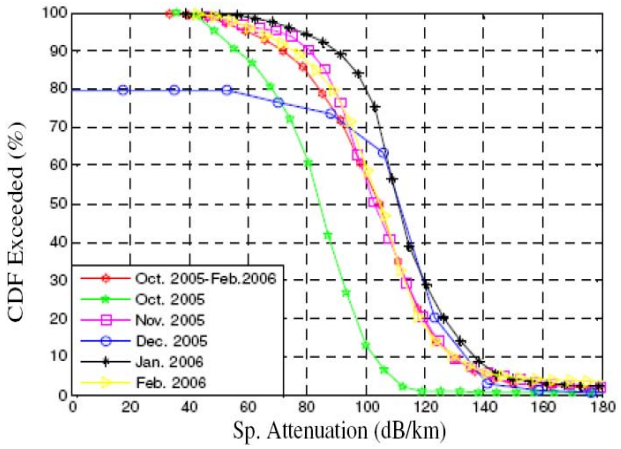

Fig. 14: Moderate continental fog at Graz showing monthly CDF exceeded (%)

This plot clearly shows that the specific attenuations are comparatively higher in January 2006 as compared to the other months. Whereas October 2005 shows relatively lower values of signal attenuations since normally in October fog starts to evolve due to favourable meteorological conditions. In the months of December and January usually the air remains saturated enough most of the time with enough cooling such that relatively dense continental fog accumulates, as is clearly evident from the Fig. 14 plot. More detailed seasonal attenuation behaviour of continental fog can be seen from the plot as shown in Fig. 15 for the Milan (Italy) case.

Milan is a big city and has an urban continental environment. The continental fog attenuation data is of two years (i.e., Apr. 2004 – Mar. 2006) for Milan. The attenuation data is for 785 nm optical wavelength transmitted on a 319 m FSO link. The optical signal attenuations are greater than 30 dB/km for about 1 % and are greater than 60 dB/km for about 0.3 % of the yearly time. Similar attenuation behaviour like Graz can be noticed for the Milan's case as the specific attenuations are highest for the month of January and are lowest in comparison for the month of June. Moreover, attenuations

are very low in comparison from April to September than from October to March. This suggests variable achievability of availability and QoS figures for terrestrial FSO link corresponding to seasonal dependence of continental fog attenuation behaviour.

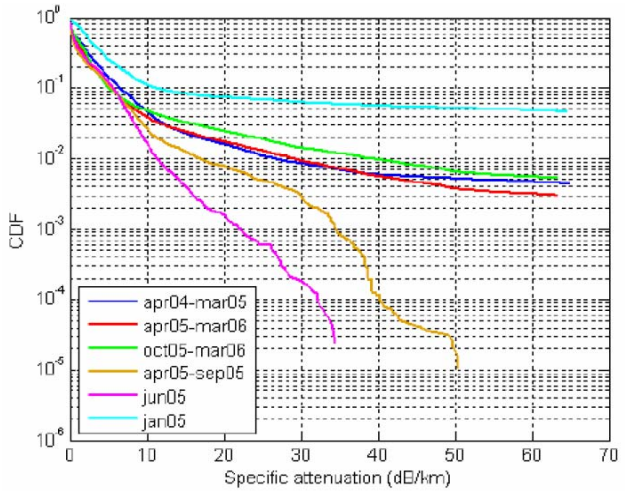

Fig. 15: CDF of fog attenuations at Milan [23]

Observing the seasonal dependence of continental fog attenuation behaviour, studying its diurnal behaviour would reveal more interesting observations. We analyse the diurnal behaviour of continental fog attenuation values from Graz data, measured on a minute scale, for four non-overlapping time intervals of 6 hour each i.e., 00:00-06:00, 06:00-12:00, 12:00-18:00, and 18:00-24:00. The plot showing diurnal variations based behaviour of continental fog attenuations is presented in Fig. 16. We can see sufficiently higher attenuations in the evening and night hours in comparison to the early and late morning hours. The attenuations are highest during time interval of 18-24 hours and the least in 00-06 time interval as compared to other three six hour intervals. We can safely term 18-24 hour interval as the worst time interval in terms of continental fog attenuations.

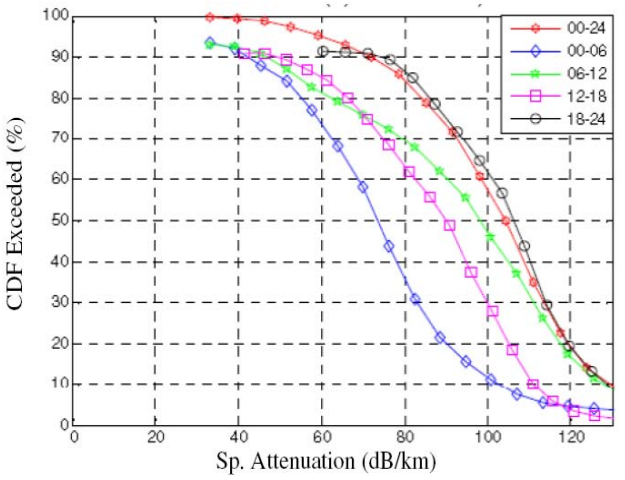

Fig. 16: Diurnal variations of moderate continental fog at Graz against CDF exceeded (%)

Since changes in continental fog attenuations occur at ± 6 dB/km averaged on a second scale, it would be interesting to study their behaviour statistically. We present in Table VII the statistics of changes in specific attenuation for the attenuation data measured on a second scale and then averaged on a minute scale for a representative fog event of 02nd February 2006 that showed a maximum attenuation of 224 dB/km.

TABLE VII

STATISTICS OF CHANGES IN SPECIFIC ATTENUATIONS (DB/KM) FOR A PARTICULAR FOG EVENT OF 2ND FEB. 2006 FOR GRAZ.

Average (sec)	Average (min)	Median (sec)	Median (min)	Maximum (sec)	Maximum (min)
± 0.000171	± 0.010715	0	± 0.010934	± 83.426	± 63.27

We noticed a maximum change of ± 83.42 dB/km in specific attenuations on a second scale for this representative fog event. By averaging it on a minute scale we get ± 63.27 dB/km change.

TABLE VIII

CUMULATIVE EXCEEDANCE PROBABILITY OF CHANGES IN SPECIFIC ATTENUATIONS UNDER CONTINENTAL FOG CONDITIONS.

Minutes Scale			Seconds Scale		
Attenuations ≥ ± 20 dB/km	Attenuations ≥ ± 10 dB/km	Attenuations ≥ ± 5 dB/km	Attenuations ≥ ± 20 dB/km	Attenuations ≥ ± 10 dB/km	Attenuations ≥ ± 5 dB/km
8.60 %	22.79 %	40.23 %	3.817 %	3.827 %	3.941 %

In Table VIII, we summarised the observed cumulative exceedance probability statistics of changes in specific attenuations for all 23 measured fog events at Graz. We find that changes in specific attenuations are ≥ 5 dB/km for about 3.941 % and 40.23 % of the time on second and minute scales, respectively.

Similarly, we investigate the behaviour of snow attenuations measured on the 80 m FSO link at Graz in terms of CDF exceeded percentage. So we plotted in Fig. 17, CDF exceeded (%) against specific attenuations measured on a second scale, for the three snow events (as presented in Fig. 12 before).

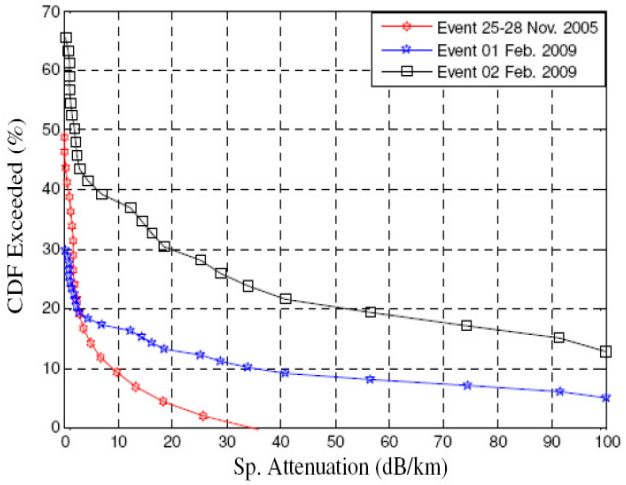

Fig. 17: Cumulative exceedance percentage of three observed snow events

We observe that CDF exceeded (%) for the 2nd Feb. 2009 shows overall high values as compared to the other two snow events of 01st Feb. 2009 and the 25-28th Nov. 2005. We observe that attenuations exceed 30 dB/km for about 2 %, 11 % and 27 % against snow events of 25-28th Nov. 2005, 01st Feb. 2009 and 2nd Feb. 2009, respectively. We find that peak value of snow attenuations can vary from event to event, at a particular location, as it depends upon the snowfall intensity and the size of the individual snowflake. If higher the snowfall rate or larger the snowflake size, it means more poor the visibility range and consequently higher get the attenuations.

We calculated the cumulative exceedance percentage of changes in specific attenuations for the three snow events and the statistics are shown in Table IX below. We summarise these statistics in terms of CDF exceeded (%) for changes in attenuations observed on a second scale, averaged on a minute and hourly scales.

TABLE IX

CUMULATIVE EXCEEDANCE PROBABILITY OF CHANGES IN SPECIFIC ATTENUATIONS UNDER SNOW CONDITIONS AT GRAZ

Seconds		Minutes		Hours	
Attenuations ≥ ± 5 dB/km	Attenuations ≥ ± 2 dB/km	Attenuations ≥ ± 5 dB/km	Attenuations ≥ ± 2 dB/km	Attenuations ≥ ± 4 dB/km	Attenuations ≥ ± 2 dB/km
0.091 %	1.274 %	0.555 %	1.052 %	29.52 %	49.53 %

We observed changes in specific attenuations for the 25-28th Nov. 2005 snow event to be around ± 10 dB/km on a second scale [24], whereas they are about ± 7 dB/km and ± 6 dB/km for 01st Feb. 2009 and 2nd Feb. 2009 snow events, respectively. The specific attenuations observed for snow events case vary at a much slower rate on a second scale when compared specific attenuations in continental fog case. And the difference in changes in attenuations between Nov. 2005 and Feb. 2009 snow events is due to the fact that the snowfall rate was very consistent and uniform in Feb. 2009 than it was in Nov. 2005.

D. Link Budget

Link budget of an optical link determines the ability to deliver the signal power from transmitter to the receiver. The main parameter for path planning is the specific margin in dependence of the link path distance. Total optical output power or receiver sensitivity is of secondary interest as long as the system meets safety regulations like an eye safe laser class. Beam divergence and acceptance angle have some practical consequences as they refer to the required mount stability and play a role in the overall installation cost. Hence, by this procedure it is possible to find a trade off between costs and effect on the received power for the optimisation of a FSO transmission system. It should be noted that few assumptions have been made in order to calculate the above mentioned link budget,

- A point source transmitter is assumed.
- The intensity distribution beam profile is assumed to be isotropical but not the Gaussian.
- The extinction ratio is assumed to be 100% between bright and dark states.

Influences of component degradation and aging, pointing loss and ambient conditions are ignored. The system properties are expressed by the virtual system power figure P_{SYS},

$$P_{SYS} = P_{TX} + G_{TX} + A_{RX} - \sum a_{SYS} \tag{11}$$

P_{TX} represents the total average optical power output power in dBm, which can be calculated from the absolute value by Eqn. 12 below,

$$P_{TX}(dBm) = 10\log\left[\frac{P_{TX}(mW)}{1mW}\right] \tag{12}$$

Divergence α of the transmitted beam (full angle) is used to calculate a geometrical gain in comparison to an isotropic source which emits omni-directional in the complete spatial angle 4π. If the divergence is given in milliard units, it can be recalculated to degrees by the formula,

$$\alpha(^\circ) = \frac{180^\circ}{1000\pi} \cdot \alpha_{[mrad]} \tag{13}$$

For the case of a circular beam the plane angle α of beam divergence can be recalculated to the corresponding spatial angle Ω using Eqn. 14,

$$\Omega = 2\pi \cdot \left(1 - \cos\frac{\alpha}{2}\right). \tag{14}$$

The geometrical gain G_{TX} can then be calculated by,

$$G_{TX}(dB) = 10\log\left(\frac{4\pi}{\Omega}\right). \tag{15}$$

Output power and transmitter gain are often referred as the effective isotropically radiated power, EIRP, describing the transmitter properties only. Assuming a single circular receiver optic (radius R in meters), the receiver aperture A_{RX} and link distance d_L contribute with the following decibel values,

$$A_{RX} = 20\log\left(R_{Optic}\right) \tag{16}$$

$$D_{Link} = 20\log\left(2d_L\right). \tag{17}$$

Where d_L is the link path distance between transmitter and receiver. Neglecting the atmospheric attenuation the received average optical power P_{RX} after d_L (m) is,

$$P_{RX}(dBm) = P_{SYS} - D_{Link} = P_{SYS} - 20\log(2d_L) \tag{18}$$

The link margin M_{SYS} (dB) for an installed system to compensate all atmospheric path losses is,

$$M_{SYS} = P_{SYS} - P_{RS} - D_L \tag{19}$$

Where P_{RS} is the receiver sensitivity limit for correct operation. Finally, the specific link margin in dB/km, dependent on the link path distance is,

$$M_{SPEC}(d_L) = \frac{1000m}{d_L}.M_{SYS} = \frac{1000m}{d_L}.[P_{SYS} - P_{RS} - D_{Link}] \qquad (20)$$

Based on the above mentioned procedure, link budget is calculated for the FSO link installed at Graz. It is shown in tabular form in Table X below.

Table X

FSO link budget using On-Off keying (OOK) for three FSO links at Graz

Parameter	80 m FSO Link	650 m FSO Link	2700 m FSO Link
PTX power (dBm)	6.0206	6.0206	6.0206
PTX power (Watt)	0.0040	0.0040	0.0040
TX Wavelength	950 nm	950 nm	950 nm
TX Gain (dB)	97.3782	97.3782	97.3782
Free Space Loss (dB)	180.4915	198.6880	211.0570
RX gain	109.2439	109.2439	109.2439
RX power (dBm)	25.1512	6.9548	-5.4142
RX power (Watt)	0.3274	0.0050	2.8746×10^{-4}
Power needed (Watt)	0.1641	0.0025	1.4407×10^{-4}
Achievable data rate (kbits/s)	2.6161×10^{12}	3.9628×10^{10}	2.2967×10^{9}

It is evident from Table X, that very high data rates are achievable in clear sky conditions with the mentioned transmit and receive parameters. But it's only the optics and electronics available that limits the achievable data rates up to 2.5 Gbps now. Moreover, the FSO link availability can only be determined through observation of BER measurements in critical weather conditions (like fog, snow and clouds) to see if they are within the acceptable limits ($< 10^{-9}$). More importantly the FSO link availability must be defined in consideration to the installed link location, climatic variability and the localised weather characteristics at that particular location. In this regard, long term measured localised weather related attenuation data is very crucial for establishing realistic availability metrics for network planning.

V. CONCLUSIONS

In this paper we reviewed the continental fog microphysics and the mechanics of fog formation and dissipation from FSO perspective. We investigated continental fog and dry snow attenuations experimental data collected on 80m FSO link installed at Graz in comparison to their particle and flake density, respectively. The measurement of density profiles corresponding to fog and snow events gives us very useful information about fog and dry snow intensity and expected levels of optical attenuations. Based on observed relative humidity, temperature and specific attenuation values, for the FSO link case, we proposed a simple empirical model to predict optical attenuations in case of continental fog that showed strong correlation with the temperature and relative humidity. Further we investigated the challenges imposed on the design and performance of terrestrial FSO links by investigating the influence of dry snow and continental fog conditions theoretically and empirically. Finally we presented a realistic link budget for FSO links for three short distance terrestrial links. We characterised optical attenuations in fog and dry snow conditions based on cumulative probability statistics. This characterisation provides interesting insight to fade margin design for terrestrial optical links. Considerable seasonal and diurnal dependence have been reported especially for continental fog case that can have a significant impact on FSO link availability. It is imperative to adjust fade margin to seasonal and diurnal variations in order to improve the availability in critical conditions like dense fog and snow. We observed especially in continental fog case that there exist strong differences between summer months and winter months, as well as between different daytimes. These observed variations in attenuations may invigorate the use of more advanced fade countermeasures. More measurement data for dry snow attenuations is required in order to characterise it more precisely and to study its seasonal and diurnal attenuation patterns for certain locations.

REFERENCES

[1] C. C. Davis, I. I. Smolyaninov and S. D. Milner, "*Flexible optical wireless links and networks*", IEEE Communication Magazine, pg. 51-57, March 2003.

[2] E. Leitgeb, M. Gebhart, A. Truppe, U. Brinbacher, P. Schrotter and A. Merdonig, "*Hybrid wireless networks for Civil-Military-Cooperation (CIMIC) and disaster management*", Proceedings of the SPIE, Vol. 5614, pp. 139-150 (2004).

[3] A. K. Majumdar and J. C. Ricklin, "*Free-Space Laser Communications, Principles and advantages*", Springer Science LLC, 2008.

[4] Nicolas Perlot, "*Characterization of signal fluctuations in optical communications with intensity modulation and direct detection through the turbulent atmospheric channel*", Ph. D thesis, 2005.

[5] J. C. Juarez, A. Dwivedi, A. R. Hammons, S. D. Jones, V. Weerackody and R. A. Nichols, "*Free-Space Optical Communications for Next-Generation Military Networks*", IEEE Communication Magazine, pg. 46-51, November 2006.

[6] D. Giggenbach, J. Horwath and B. Epple, "*Optical Satellite Downlinks to Optical Ground Stations and High-Altitude Platforms*", IST Mobile & Wireless Communication Summit, Budapest, Hungary, July 2007.

[7] H. Hemmati, "*Deep Space Optical Communications*", John Wiley & Sons, 2006.

[8] Fredrick G. Smith, "*Atmospheric Propagation of Radiation Volume 2, The infrared and electro-optical systems handbook*", SPIE, 1993.

[9] M. Akiba, K. Wakamori and S. Ito, "*Measurement of optical propagation characteristics for free-space optical communications during rainfall*", IEICE Transactions on Communications E87-B, 2053-2056 (2004).

[10] Sajid S. Muhammad, B. Flecker, E. Leitgeb and M. Gebhart, "*Characterization of fog attenuation in terrestrial free space optical links*", Journal of OE 46(4) 066001 June 2007.

[11] L. Castanet, "*Influence of the variability of the propagation channel on mobile, fixed multimedia and optical satellite communications*", JA2410 SatNEx e-book, Shaker Verlag 2007.

[12] R. Nebuloni and C. Capsoni, "*Laser attenuation by Falling Snow*", CSNDSP 2008, 23-25 July 2008, Graz, Austria.

[13] Art MacCarley, "*Advanced Image Sensing for Traffic Surveillance and Detection*", California PATH Research Report, 1999.

[14] M. Gebhart, E. Leitgeb, S. Sheikh Muhammad, B. Flecker, C. Chlestil, M. Al Naboulsi, H. Sizun and F. De Fornel, "*Measurement of light attenuation in dense fog conditions for optical wireless links*", SPIE proceedings, Vol. 589, 2005.

[15] Van de Hulst, "*Light scattering by small particles*", New York, Dover Publications, 1981, 470 p., ISBN 0486642283.

[16] C. F. Bohren and D. R. Huffman, "*Absorption and scattering of light by small particles*", John Wiley and sons, New York, 1983, ISBN 0471293407, ISBN 9780471293408.

[17] V. Kvicera, M. Grabner, and O. Fiser, "*Attenuation Due to Hydrometeors at 850 nm Measured on an 850 m Path*", WOC 2008, Quebec, Canada.

[18] H. W. O'Brien, "*Visibility and Light Attenuation in Falling Snow*", Journal of Applied Meteorology, vol. 9, pp. 671-683, 1970.
[19] D. Atlas, "*Shorter Contribution Optical Extinction by Rainfall," J. Meteorology*", Vol. 10, pp. 486-488, 1953.
[20] ITU recommendation ITU-R P. 1622, "*Prediction methods required for the design of Earth-space systems operating between 20 THz and 375 THz*".
[21] S. Arnon D. Sadot, and N. S. Kopeika, "*Simple mathematical models for temporal, spatial, angular, and attenuation characteristics of light propagating through the atmosphere for space optical communication: Monte Carlo simulations*", Journal of Modern Optics, Vol. 41, No. 10, pp. 1955-1972, 1994.
[22] M. Akiba, K. Ogawa, K. Wakamori, K. Kodate and S. Ito, "*Measurement and simulation of the effect of snowfall on free-space optical propagation*", Journal of Applied Optics, Vol. 47, No. 31, pp. 5736-5743, 01 Nov. 2008.
[23] C. Capsoni and R. Nebuloni, "*Optical Wave Propagation through the Atmosphere in a Urban Area*", Mediterranean Microwave Symposium 2006, Genova, Italy, 19-21 September, 2006, pp. 335-338.
[24] B. Flecker et. Al, "*Results of measurements for optical wireless channels under dense fog conditions regarding different wavelengths*", SPIE Proceedings, Vol. 6303, 63030P, 2006.

Muhammad Saleem Awan received his M. Sc. Physics with specialisation in Electronics degree from Government College Lahore, Pakistan in 1996. In January 2007, he started his Ph. D research in the area of Optical Wireless at Graz University of Technology. His current interests include optical wireless communication channel modelling, wireless technologies and satellite communication. He is actively involved in international projects like European Satellite Communications Network of Excellence (SatNEx) work package on *Clear Sky Optics*, ESA project on *Feasibility Assessment of Optical Technologies & Techniques for Reliable High Capacity Feeder Links* and COST action IC0802 on *Propagation tools and data for integrated Telecommunication, Navigation and Earth Observation systems*.

László Csurgai-Horváth received the M.Sc. degree in electrical engineering from Budapest University of Technology and Economics (BME) in 1985. Currently he is employed as research engineer at BME, Department of Broadband Infocommunications and Electromagnetic Theory. His current research interests focused on microwave propagation, stochastic modeling of rain and multipath propagation attenuation on terrestrial and satellite radio links and time series synthesis. One of his recent topics include the impact of precipitation in the free space optical and 50-90 GHz band radio wave propagation. He was involved in several national and international research projects and also author of more than 30 journal and conference publications.

Dr. Sajid Sheikh Muhammad did his Bachelors and Masters in Electrical Engineering in 2001 and 2003 from the University of Engineering and Technology, Lahore, Pakistan. and his in Electrical Engineering in 2003 from the same University where he also remained in the faculty from 2002 to 2004. He moved to Graz University of Technology in 2004 to pursue his doctoral research and completed his PhD with Excellence in 2007 having contributed significantly to the channel modeling and coded modulation design for FSO links. During the course of his PhD, he remained active within many European Union projects particularly the SatNEx, COST 270 and an ESA study. He has published over 30 articles in peer-reviewed International conferences and Journals and act as reviewer and international technical committee member to numerous conferences and journals in the area of Optical wireless communications. He organized the First IEEE Colloquium on Optical Wireless Communications at the CSNDSP 2008 in Graz, Austria whereby 27 contributions from around the globe were presented. He was recently approved as a Non-COST country representative for the new COST action IC0802. He is working as an Assistant Professor at the National University of Computer and Emerging Sciences (FAST-NU) in Lahore, Pakistan since Fall 2007, where he lectures on Communication System Design, Wireless Communications, Optical Fiber Communications and Coding Theory. His main research interest lies in optical wireless communications, channel modeling and the application of Coding and Information theory to optical wireless systems.

Erich Leitgeb received his MS in electrical engineering at TU Graz in 1994. In 1994, he started research work in optical communications at the Department of Communications and Wave Propagation at TU Graz. In February 1999, he received his PhD with honors. Since January 2000, he has been the project leader of international research projects (COST 270, SatNEx and ESA) in the field of optical wireless communications. He established and leads the research group for optical communications at TU Graz. He is currently an assistant professor at the TU Graz. He gives lectures in optical communications engineering, antennas and wave propagation, and microwaves. He is a member of IEEE, SPIE, and WCA. Since 2003, he has been a reviewer for IEEE and SPIE conferences and journals and acts as member of technical committees and chairperson on conferences.

Farukh Nadeem was born in 1968 in Khair Pur Mir's, Pakistan. He obtained his M.Phil in Electronics in 1996 from Quaid-e-Azam University Islamabad, Pakistan. He joined a public sector research and development organization based in Islamabad in April 1996. He worked on different electronics research projects. His current field of interest is the intelligent switching of free space optical / RF communication links, a field in which he is pursuing a PhD since Feb, 2007. He is actively participating in international projects, such as SatNEx (a network of excellence with work package on "clear sky optics"), ESA project (Feasibility Assessment of Optical Technologies & Techniques for Reliable High Capacity Feeder Links) and COST action IC0802 (Propagation tools and data for integrated Telecommunication, Navigation and Earth Observation systems).

Muhammad Saeed Khan received his M. Sc Electronics degree in 2004 from Quaid-E-Azam University, Islamabad, Pakistan. He worked as a lecturer from Sept. 2004 to Feb. 2006 at the Department of Physics and Electronics at COMSATS Institute of Information Technology, Wah Cantt, Pakistan. Since April 2006, he has been working towards his PhD at the Graz University of Technology (TU Graz), Austria, in the area of optical wireless communication. His research interests are channel estimation, channel modeling and channel characterization for terrestrial optical wireless links.